The formin FHOD1 in cardiomyocytes

Joseph Dwyer1, Marlene Pluess1, Thomas Iskratsch1,2, Cristobal G. dos Remedios3 and Elisabeth Ehler1

1 Randall Division of Cell and Molecular Biophysics and Cardiovascular Division, British Heart Foundation Centre of Research Excellence, King's College London, London SE1 1UL, UNITED KINGDOM
2 Columbia University, Biological Sciences, 713 Fairchild Center, New York, NY 10027, USA
3 Bosch Institute, Department of Anatomy, University of Sydney, Sydney 2006, Australia

Corresponding author: Dr Elisabeth Ehler
Room 3.26A
Randall Division of Cell and Molecular Biophysics
King's College London
New Hunt's House
Guy's Campus
London SE1 1UL
UNITED KINGDOM
Phone ++44 20 7848 6067
Fax ++44 20 7848 6435
Email Elisabeth.ehler@kcl.ac.uk

Keywords: formin, actin, intercalated disc, sarcomere

Abbreviations: DAD Diaphanous autoregulatory domain, DCM dilated cardiomyopathy, DID Diaphanous inhibitory domain, FH formin homology domain, GBD GTPase binding domain, NRC neonatal rat cardiomyocyte

Abstract

Members of the formin family are known to be involved in the regulation of the actin cytoskeleton. We have recently identified a muscle specific splice variant of the formin FHOD3 and demonstrated its role in the maintenance of the contractile filaments of cardiomyocytes. Here we characterise the expression and subcellular localisation of FHOD3's closest relative, FHOD1, in the heart. Confocal microscopy shows that FHOD1 is mainly located at the intercalated disc, the special type of cell-cell contact between cardiomyocytes, but also partially associated with the myofibrils. Subcellular targeting of FHOD1 is probably mediated by its N-terminal domain, since expression constructs lacking this domain show aberrant localisation in primary cultures of neonatal rat cardiomyocytes. Finally we show that in contrast to FHOD3, FHOD1 shows increased expression levels in dilated cardiomyopathy, suggesting that the two formins play distinct roles and are differentially regulated in cardiomyocytes.

Introduction

Cardiomyocytes, which make up the bulk of heart mass, are characterised by an exquisitely organised cytoskeleton, which is the basis of maximal functional output (Ehler, 2010). The actin cytoskeleton comprises the thin filaments in the myofibrils, which mediate muscle contraction together with the thick (myosin) filaments, but in addition plays also a role in the organisation of the plasma membrane cytoskeleton as well as in the anchoring of myofibrils at the specialised type of cell-cell contact in heart tissue, the intercalated disc (Dwyer et al., 2012). Despite this crucial role of actin in the function of cardiomyocytes, it is subjected to an impressive amount of protein turnover. Measurements in rat hearts have suggested that actin has a half-life of about 10 days (Martin, 1981). How the exchange of actin molecules is achieved in the continuously working cardiomyocyte is not well understood.

We have recently focused our attention on a potential role of formins in the heart. Formins are proteins, which are mainly involved in the formation of linear actin filaments (Chesarone et al., 2010). They are characterised by the possession of an FH1 and an FH2 domain (for domain layout of formins see Figure 1), which together make up the actin capturing and polymerisation machinery and so far 15 different formins were described in mammals (Schönichen and Geyer, 2010).

One characteristic of formins is that they normally exist in an autoinhibited state, which is brought about by an intramolecular interaction between the N-terminal DID and the C-terminal DAD domain. Binding of a small GTPase

within the N-terminus and/or phosphorylation of the C-terminus by ROCK were documented as being prerequisites in the activation of these molecules (Chesarone et al., 2010).

One of the formins, Daam1, was shown to be crucial for early heart development (Li et al., 2011) and we have recently demonstrated that another one, FHOD3, is required for myofibril maintenance (Iskratsch et al., 2010). FHOD3 exists in several splice variants, one of which is subject to regulation by CK2 phosphorylation and is expressed exclusively in striated muscle (Katoh and Katoh, 2004; Iskratsch et al., 2010). Interestingly, the downregulation of the expression of this isoform accompanies the phenotype of murine and human dilated cardiomyopathy (Iskratsch et al., 2010).

The closest relative of FHOD3, FHOD1 has so far mainly been studied in cultured cells. It was initially shown to be involved in stress fibre formation as well as in plasma membrane blebbing (Gasteier et al., 2003; Hannemann et al., 2008). In addition, FHOD1 was shown to activate transcription from the serum responsive element (Westendorf, 2001). More recently it was demonstrated that FHOD1 may actually have more an actin bundling than a classical nucleating activity (Schönichen et al., 2013). Furthermore its role in cell spreading and adhesion maturation was discovered recently (Iskratsch et al., 2013a). Studies in smooth muscle have shown that FHOD1 is involved in the regulation of differentiation and that high levels of expression are required to maintain the expression of smooth muscle marker proteins (Staus et al., 2011). In that study, analysis of the tissue expression of FHOD1 demonstrated high levels in bladder and stomach, low levels in aorta and in

skeletal muscle and no expression in the heart (Staus et al., 2011).
Our own analysis of heart tissue using several different antibodies demonstrate that FHOD1 is expressed in cardiomyocytes at similar levels as in skeletal muscle and that it is mainly located at the intercalated disc. In analogy to many other formins our data indicates that FHOD1's subcellular targeting is mediated by its N-terminal domain. In contrast to our observations for FHOD3, we find increased expression levels of FHOD1 in dilated cardiomyopathy, suggesting diverging roles and regulation of those two formins.

Material and Methods

Murine and human samples

Adult male C57/BL6 wild type and MLP$^{-/-}$ mice (Arber et al., 1997) were used for tissues in Western Blot analysis and immunofluorescence studies. Experiments were performed in accordance with the Guidance on the Operation of Animals (Scientific Procedures) Act, 1986 (UK). Prior to harvesting tissues, mice were sacrificed by cervical dislocation. Tissues for cryosectioning were snap frozen in methylbutane in liquid nitrogen. For SDS samples, tissues were frozen in liquid nitrogen, pulverised, and lysed in SDS lysis buffer (130mM Tris, 190mM SDS, 3.69M urea, 0.06% NP40, 0.17%β-mercaptoethanol, 3.85% glycerol and 0.01% bromphenol blue at pH 6.8)

(Iskratsch et al., 2010). For immunofluorescence staining, the hearts were sectioned on a Leica CM1950 cryostat (Leica, Wetzlar, Germany) into 12µm sections, mounted on poly-L-lysine coated microscope slides, fixed with pre-cooled acetone (-20°C) for 5min followed by antibody staining as described previously (Iskratsch et al., 2010).

Human specimens were obtained from The University of Sydney, Australia via St Vincent's Hospital (Hospital Research Ethical Committee approval #H03/118; University of Sydney ethical approval #12146). Human materials were used in accordance with the ethical guidelines of King's College London (College Research Ethical Committee 04/05-74; REC reference 12/EM/0106) and the current UK law.

Neonatal Rat Cardiomyocytes

Neonatal rat cardiomyocytes (NRCs) were isolated from day 1 newborn Wistar rat pups. NRCs were isolated using the Worthington Neonatal Cardiomyocyte Isolation System (Worthington Biochemical Corporation, Lakewood, NJ, USA) according to the manufacturer's instructions. Cells were seeded onto PureCol® purified bovine collagen solution (Advanced BioMatrix, San Diego, CA, USA) coated 30mm dishes in NRC plating medium and cultured and immunostained as described previously (Iskratsch et al., 2010). Transient transfections were carried out using Escort III (Sigma-Aldrich) as a transfection reagent.

Antibodies

All antibodies against FHOD1 were obtained from commercial sources. The polyclonal goat (pG) antibodies anti FHOD1 (C14; against a peptide within an internal region of FHOD1 and C20; against a peptide near the C-terminus of FHOD1) were from Santa Cruz (Dallas, TX, USA), the polyclonal mouse (pM) anti full length FHOD1 was from Abcam (Cambridge, UK) and the polyclonal rabbit (pR) anti FHOD1 Phospho-Threonine 1141 was from ECM Biosciences (Versailles, KY, USA). The pR anti-sarcomeric alpha-actinin was a kind gift from Prof. Dieter Fürst (University of Bonn, Germany). The monoclonal mouse (mM) anti-myomesin (clone B4) antibody was produced in the lab (Grove et al., 1984) and the mM anti sarcomeric alpha-actinin (clone EA-53) was purchased from Sigma (Dorset, UK). The mM anti GFP (clones 7.1 and 13.1) was bought from Roche (Burgess Hill, UK). The pR anti-NRAP antibody was generated by immunisation of rabbits with a peptide portion of NRAP by Bioscience (Göttingen, Germany). All Cy-conjugated secondary antibodies were purchased from Jackson Immuno Research (West Grove, PA, USA) and only multi-labelling quality antibodies were employed. The anti mouse HRP-conjugated secondary antibodies were purchased from DAKO (Glostrup, Denmark) and the anti rabbit HRP-conjugated secondary antibodies were purchased from Chemicon (via Merck-Millipore, Billerica, MA, USA). DAPI was obtained from Sigma and Alexa633-phalloidin was purchased from LifeTechnologies (Paisley, UK).

Preparation of Transfection Constructs

The full length long variant of FHOD1[1-1191] was amplified from human skeletal muscle cDNA (Clontech Laboratories), using LaTaq polymerase (TaKaRa Bio, Shiga, Japan) and the appropriate primers (synthesised by Eurofins MWG Operon, Ebersberg, Germany; Accession number used for FHOD1: XM_005255909.1 in March 2008; see also (Tojo et al., 2003) and (Iskratsch et al., 2013a). FHOD1 ΔDAD [1-1096] and the FHOD1 domain constructs (FH2, GBD-DID, GBD, and DID) were amplified using the full length FHOD1 [1-1191] construct DNA as a template. The following primer sets were used: FHOD1 [1-1191] fwd 5‘GGAATTCATGGCGGGCGGGGAAGAC3’, rev 3’ GGGGTACCCACCTCCAGGCCAGGACC5’; FHOD1 deltaDAD [1-1096] fwd 5‘GGAATTCATGGCGGGCGGGGAAGAC3’, rev 3'GGGGTACCGGCGATTGTGTGTGGTG5'; FHOD1-FH2 [642-1031] fwd 5’ GGAATTCGACAGCTCAGCCCTCCCC3’, rev 3’GGGGTACCGGCGATTGTGTGTGGTG5’; FHOD1-GBD [1-116] fwd 5‘GGAATTCATGGCGGGCGGGGAAGAC3’, rev 3’GGGGTACCAAGATAGCGTTGACCCTC5’; FHOD1-GBD-DID [1-340] fwd 5’GGAATTCATGGCGGGCGGGGAAGAC3’, rev 3’GGGGTACCTTCTTCGATGTCTCCATC5’; FHOD1 DID [117-340] fwd 5’GGAATTCTACCCAGCTCTCTGTGAGG3’, rev 3’GGGGTACCTTCTTCGATGTCTCCATC5’. The DNA fragments amplified from PCR were cloned into the pEGFP-C1 and pEGFP-C2 (Clontech/TaKaRa

Bio, Shiga, Japan) vectors for eventual expression as N-terminally tagged green fluorescent fusion proteins via the EcoRI and KpnI sites. All constructs were verified by sequencing (Eurofins MWG Operon, Ebersberg, Germany). Verification of correct expression of the constructs was additionally carried out by transiently transfecting COS cells using Escort IV as a transfection reagent and analyzing the molecular weight of the GFP-fusion proteins by immunoblots as described below.

SDS-PAGE and immunoblotting, immunofluorescence and confocal microscopy

Sample preparation, SDS-PAGE and immunoblotting were all performed as described previously (Iskratsch et al., 2010). Immunoreactions on the blots were visualised by chemiluminescence using horse radish peroxidase-conjugated secondary antibodies against mouse or rabbit immunoglobulins and the signal was detected either conventionally with X-ray films or using a Fusion Solo Detector (Vilber Lourmat, Marne La Vallee, France). Immunostaining of frozen sections and fixed neonatal rat cardiomyocytes were all carried out as before (Iskratsch et al., 2010). All confocal microscopy was performed on a LSM510 laser scanning confocal microscope (Carl Zeiss MicroImaging GmbH, Jena, Germany) or an SP5 laser scanning confocal microscope (Leica Microsystems, Mannheim, Germany) with solid state (diode) laser excitation at 405 nm and emission at 420-480 nm, Ar-laser excitation at 488 nm and emission at 505-530 nm or He-Ne-laser excitation at

546 and 633 nm and emission at 560-615 nm and > 650 nm using Plan-Apochromat 63x/1.4 oil objectives or Plan-Neofluar 40x/0.9 oil objectives. Digital images were processed and assembled to figures in Photoshop (Adobe Systems, San Jose, CA, USA).

Results

In order to investigate the expression of FHOD1 at tissue level, we performed immunoblots with FHOD1 specific antibodies. We used only commercially available antibodies, however, due to the high levels of homology between forming family members and based on potential cross-reactivity of polyclonal antisera with other muscle proteins (for example see Wang et al., 2012), we decided to evaluate the specificity of our reagents first. Immunocytochemistry and immunoblots on COS cells that were transiently transfected with FHOD1 and FHOD3 constructs clearly showed that the anti FHOD1 antibodies that we used only recognised FHOD1 and did not cross-react with FHOD3 (Figure 2A, B). The antibody (pR anti FHOD1 pThr1141) that was used for most of the immunohistochemistry experiments was additionally evaluated on NRC overexpressing full length and C-terminally truncated FHOD1 (FHOD1-deltaDAD) and while it gave a clear signal for full length FHOD1 it failed to detect the C-terminally truncated version, which lacks Thr1141 (Figure 3). In addition, the antibody did not pick up any cross-striated pattern in the NRC, suggesting that it does not cross-react with well-known problematic proteins

such as sarcomeric alpha-actinin or sarcomeric myosin (Figure 3). We therefore proceeded to study FHOD1 expression by immunoblot on whole muscle samples from mouse. As expected, a prominent band was seen in spleen (Westendorf et al., 1999; Tojo et al., 2003), which was used as a positive control, but a band of the same molecular weight was also detected in heart, as well as in fast and slow twitch skeletal muscle (Tibialis anterior, TA, and Soleus, respectively, Figure 4). Expression of sarcomeric alpha-actinin was used as a loading control and suggested that expression of FHOD1 is higher in heart and fast twitch than in slow twitch muscle. To investigate the subcellular localisation of FHOD1, immunohistochemistry on frozen sections followed by confocal microscopy analysis was performed. With three different FHOD1 antibodies that are directed against three different epitopes along the molecule, a strong signal was seen in cardiomyocytes, which was mainly concentrated at the specific sites of cell-cell contact in heart, the intercalated discs (Figure 5). Occasionally a cross-striated pattern was seen, suggesting some association of FHOD1 with myofibrils. Counterstaining for the M-band marker myomesin revealed alternating striations and indicates that FHOD1 may be present in some of the Z-discs. Interestingly this localisation pattern may be evolutionally conserved, since also C. elegans FHOD1 is found as bright puncta at the muscle cell edges with faint striations at the dense bodies, the equivalent of the Z-disc (Mi-Mi et al., 2012). The three different antibodies revealed grossly similar staining patterns in heart sections and also the signal with the antibody that is expected to detect only active FHOD1, which is phosphorylated on Threonine 1141, looked comparable to the results

obtained with the antibodies that detect all FHOD1 (compare Figure 5C with A, B). Together these results demonstrate FHOD1 expression in cardiomyocytes, where it is predominantly found at the intercalated disc.

Next we wanted to analyse the effect of overexpression of FHOD1 on the cytoarchitecture of primary cultures of neonatal rat cardiomyocytes (NRC). Expression tests of the GFP-tagged constructs in transiently transfected COS cells followed by immunoblotting revealed that GFP fusion proteins of the expected molecular weight were generated and that also the expression levels are roughly similar between constructs, apart from lower expression levels for the C-terminal deletion construct (deltaDAD; Figure 6). Transient expression of full length and constitutively active (by means of truncation of its C-terminal DAD domain) GFP-tagged FHOD1 was carried out in NRC and the effect on the myofibrils and the actin cytoskeleton was investigated by confocal microscopy. Full length FHOD1 again shows a predominant localisation at the periphery of the cells (Figure 7A). In addition, there was a lot of diffuse cytoplasmic signal with hardly any visible signs of cross-striations. No increased signal was seen at the cell-cell contacts between the NRC. Overexpression of constitutively active FHOD does not seem to affect the organisation of the myofibrils as indicated by their sarcomeric alpha-actinin signal. However, there was evidence for increased levels of filamentous actin, compared to untransfected control cells (Figure 7B). This suggests that while overexpression of full length FHOD1 is well tolerated and has little effect on cytoarchitecture, increased expression of active FHOD1 may lead to increased actin filament formation, similar to observations that

were made using constitutively active FHOD3 (Iskratsch et al., 2013b).

The subcellular targeting of formins is often mediated by their N-terminus (Seth et al., 2006; Ramalingam et al., 2010), which also tends to be the part of the molecule with the highest divergence in its sequence and even in its structure (Schulte et al., 2008). We created GFP-tagged expression constructs that only encoded for subdomains of FHOD1 and analysed their subcellular targeting in NRC. The FH2 domain of FHOD1 on its own displays a strong signal at the Z-disc, as indicated by its alternation with signal for the M-band protein myomesin (Figure 8A). Constructs encoding the GBD-DID domain or even only the GBD domain on its own show mainly diffuse cytoplasmic localisation with some evidence for myofibril association (Figure 8B, D; for scheme of the constructs see Figure 1). DID alone as well as an N-terminal deletion construct lacking the GBD domain either showed aggregates or small vesicular-like structures. These experiments suggest that the GBD domain of FHOD1 mediates the subcellular targeting that is observed for full length FHOD1 in NRC.

Our previous studies had demonstrated that the expression of the closest relative of FHOD1, FHOD3, is downregulated in dilated cardiomyopathy (Iskratsch et al., 2010). Interestingly this was not seen when the expression of FHOD1 was analysed in MLP knockout mice, a mouse model for dilated cardiomyopathy (Arber et al., 1997). In fact the signal of FHOD1 at the intercalated disc even seems to be increased, in a similar way to the signal for N-RAP, which was previously shown to be an early marker for dilated cardiomyopathy (Figure 9A; Ehler et al., 2001). This increase in FHOD1

expression could also be reproduced in human DCM samples compared to controls (Figure 9B). Therefore, the formins FHOD1 and FHOD3 seem to play distinct roles in DCM, one being up- the other being downgulated.
In conclusion we have demonstrated that the formin FHOD1 is expressed in heart and that it localises mainly at the intercalated disc. In DCM the signal for FHOD1 at the intercalated discs is increased, probably due to increased membrane convolution and may indicate a potential role of FHOD1 in the formation of actin anchoring structures.

Discussion

This study focused on the formin FHOD1 and shows its expression and subcellular localisation in cardiomyocytes. Previous studies had cast doubt on the expression of FHOD1 in heart (Staus et al., 2011), but we show here with several different antibodies that we can visualise FHOD1 in cardiomyocytes and get consistent results. Since we have validated the reactivity of these antibodies and their lack of cross-reaction with FHOD3 using expression constructs (Figure 2), we are confident that they do detect endogenous FHOD1 and that the signal is not due to a cross-reaction. Analysis of human FHOD1 expression at the mRNA level had previously suggested its presence in striated muscle tissue (reviewed in Randall and Ehler, 2013). Interestingly, slow twitch fibres appear to express lower levels of FHOD1 than either fast twitch fibres or the heart, which is in contrast to many other cytoskeletal

proteins, which seem to be regulated in their expression in a similar way in ventricular and slow twitch muscle (Schiaffino and Reggiani, 1996). Overexpression of FHOD1 in NRC revealed a mainly diffuse signal with major intensities at the periphery of the cells. However, in contrast to the observed localisation for FHOD1 at the intercalated disc in heart tissue, we did not detect a consistently increased signal for FHOD1 at the cell-cell contacts between NRC. These contacts are often termed intercalated disc-like structures, since although the classical intercalated disc components such as desmosomal proteins and gap junction proteins can be identified there, one major difference is that they do not necessarily have to have end-on insertion of myofibrils but can also occur in parallel to myofibrils (Hirschy et al., 2006). Analysis of FHOD1 expression during embryonic heart development and comparison of its localisation with established intercalated disc anatomy will be required to determine, whether FHOD1 is only a late addition and characterises mature intercalated discs in the three-dimensional environment in situ.

The expression of constitutively active FHOD1 induced a star-like phenotype in NRC. This is in contrast to overexpression of constitutively active FHOD3 in NRC, which lead to a massive increase in filamentous actin stretching throughout the cell (Iskratsch et al., 2013b). This observation together with the slightly different subcellular targeting and the dramatically different response of FHOD1 and FHOD3 to an insult such as dilated cardiomyopathy, highlight that despite their homology these two formins carry out distinct functions in cardiomyocytes. Their different subcellular targeting means that they regulate

distinct sets of actin filaments and their expression is also regulated independently. These observations provide further evidence for the hypothesis that formins are not general actin filament polymerising factors but carry out subtly different, tightly regulated roles, that are hugely dependent on their subcellular targeting (Randall and Ehler, 2013).

The localisation of FHOD1 at the intercalated disc and its upregulation in dilated cardiomyopathy are especially intriguing when recent findings on the role of the intercalated disc in cardiomyocyte growth are considered. Altered stoichiometry of intercalated disc proteins was suggested a decade ago to be among the hallmarks of dilated cardiomyopathy (Perriard et al., 2003) and many proteins were shown to be altered in their expression (Estigoy et al., 2009). Interestingly, proteins that are involved in the anchoring of actin filaments always tend to be increased in their expression levels (Ehler et al., 2001). The intercalated discs also attain a broader appearance, which is due to increased convolution of the contacting plasma membranes, similar to observations made in the aged heart (Forbes and Sperelakis., 1985). A recent study on a volume overload model in the rabbit has proposed the weaving sarcomere hypothesis, which means that sarcomeres are inserted at the terminals of the cardiomyocyte to increase its size, which leads to a transient splitting of the signal for intercalated disc proteins (Yoshida et al., 2010). This agrees well with the concept of the transitional junction (Bennett et al., 2006), which contains only a subset of Z-disc proteins and does not show increased electron density ultrastructurally. Via the transitional junction the actin filaments transgress with maintained polarity towards the intercalated disc

(Yamaguchi et al., 1988). Controlled insertion of sarcomeres in these regions was also documented during heart development and shown to be disturbed in dilated cardiomyopathy (Wilson et al., 2014). Increased actin anchorage together with the elevated levels of an actin nucleating and/or bundling protein such as FHOD1 may contribute to the imbalance of growth and eventually to the observed phenotypes in dilated cardiomyopathy. FHOD1 may thus not only be relevant for normal heart function but may also play a crucial role in heart disease.

Acknowledgements

This research was funded by a PhD studentship of the British Heart Foundation to JD, a Pump Priming grant from the British Heart Foundation Centre of Research Excellence at King's College London to TI and EE and a doctoral studentship from the Boehringer Ingelheim Fonds to MP. TI is the recipient of an American Heart Association fellowship.

References:

Arber S, Hunter JJ, Ross JJ, Hongo M, Sansig G, Borg J, Perriard J-C, Chien KR, Caroni P. 1997. MLP-deficient mice exhibit a disruption of cardiac

cytoarchitectural organization, dilated cardiomyopathy, and heart failure. Cell 88:393-403.

Bennett PM, Maggs AM, Baines AJ, Pinder JC. 2006. The transitional junction: a new functional subcellular domain at the intercalated disc. Mol Biol Cell 17:2091-2100.

Chesarone MA, DuPage AG, Goode BL. 2010. Unleashing formins to remodel the actin and microtubule cytoskeletons. Nat Rev Mol Cell Biol 11:62-74.

Dwyer J, Iskratsch T, Ehler E. 2012. Actin in striated muscle: recent insights into assembly and maintenance. Biophysical Reviews 4:17-25.

Ehler E. 2010. Changes at the cellular level in the diseased heart and their implications on function. Kerala, India: Transworld Research Network.

Ehler E, Horowits R, Zuppinger C, Price RL, Perriard E, Leu M, Caroni P, Sussman M, Eppenberger HM, Perriard JC. 2001. Alterations at the intercalated disk associated with the absence of muscle LIM protein. J Cell Biol 153:763-772.

Estigoy CB, Ponten F, Odeberg J, Herbert B, Guilhaus M, Charleston M, Ho JWK, Cameron D, dos Remedios C. 2009. Intercalated discs: multiple proteins perform multiple functions in non-failing and failing human hearts. Biophys Rev 1:43-49.

Forbes MS, Sperelakis. N. 1985. Intercalated discs of mammalian heart: a review of structure and function. Tissue Cell 17:605-648.

Gasteier JE, Madrid R, Krautkramer E, Schroder S, Muranyi W, Benichou S, Fackler OT. 2003. Activation of the Rac-binding partner FHOD1

induces actin stress fibers via a ROCK-dependent mechanism. J Biol Chem 278:38902-38912.

Grove BK, Kurer V, Lehner C, Doetschman TC, Perriard JC, Eppenberger HM. 1984. Monoclonal Antibodies Detect New 185,000 Dalton Muscle M-Line Protein. J Cell Biol. 98:518-524.

Hannemann S, Madrid R, Stastna J, Kitzing T, Gasteier J, Schonichen A, Bouchet J, Jimenez A, Geyer M, Grosse R, Benichou S, Fackler OT. 2008. The Diaphanous-related Formin FHOD1 associates with ROCK1 and promotes Src-dependent plasma membrane blebbing. J Biol Chem 283:27891-27903.

Hirschy A, Schatzmann F, Ehler E, Perriard JC. 2006. Establishment of cardiac cytoarchitecture in the developing mouse heart. Dev Biol 289:430-441.

Iskratsch T, Lange S, Dwyer J, Kho AL, dos Remedios C, Ehler E. 2010. Formin follows function: a muscle specific isoform of FHOD3 is regulated by CK2 phosphorylation and promotes myofibril maintenance. J Cell Biol 191:1159-1172.

Iskratsch T, Yu CH, Mathur A, Dwyer J, Liu S, Stévenin V, Hone J, Ehler E, Sheetz M. 2013a. FHOD1 is needed for directed forces and adhesion maturation during cell spreading and migration. Dev Cell 27:545-559.

Iskratsch T, Reijntjes S, Dwyer J, Toselli P, Degano IR, Dominguez I, Ehler E. 2013b. Two distinct phosphorylation events govern the function of muscle FHOD3. Cell Mol Life Sci 70:893-908.

Katoh M, Katoh M. 2004. Identification and characterization of human FHOD3 gene in silico. Int J Mol Med 13:615-620.

Li D, Hallett MA, Zhu W, Rubart M, Liu Y, Yang Z, Chen H, Haneline LS, Chan RJ, Schwartz RJ, Field LJ, Atkinson SJ, Shou W. 2011. Dishevelled-associated activator of morphogenesis 1 (Daam1) is required for heart morphogenesis. Development 138:303-315.

Martin AF. 1981. Turnover of cardiac troponin subunits. Kinetic evidence for a precursor pool of troponin-I. J Biol Chem 256:964-968.

Mi-Mi L, Votra S, Kemphues K, Bretscher A, Pruyne D. 2012. Z-line formins promote contractile lattice growth and maintenance in striated muscles of C. elegans. J Cell Biol 198:87-102.

Perriard JC, Hirschy A, Ehler E. 2003. Dilated cardiomyopathy: a disease of the intercalated disc? Trends Cardiovasc Med 13:30-38.

Ramalingam N, Zhao H, Breitsprecher D, Lappalainen P, Faix J, Schleicher M. 2010. Phospholipids regulate localization and activity of mDia1 formin. Eur J Cell Biol 89:723-732.

Randall TS, Ehler E. 2013. A formin-g role during development and disease. Eur J Cell Biol Epub ahead of print. doi 10.1016/j.ejcb.2013.11.004

Schiaffino S, Reggiani C. 1996. Molecular diversity of myofibrillar proteins: gene regulation and functional significance. Physiol Rev 76:371-423.

Schönichen A, Geyer M. 2010. Fifteen formins for an actin filament: a molecular view on the regulation of human formins. Biochim Biophys Acta 1803:152-163.

Schönichen A, Mannherz HG, Behrmann E, Mazur AJ, Kuhn S, Silvan U, Schoenenberger CA, Fackler OT, Raunser S, Dehmelt L, Geyer M. 2013. FHOD1 is a combined actin filament capping and bundling factor that selectively associates with actin arcs and stress fibers. J Cell Sci 126:1891-1901.

Schulte A, Stolp B, Schonichen A, Pylypenko O, Rak A, Fackler OT, Geyer M. 2008. The human formin FHOD1 contains a bipartite structure of FH3 and GTPase-binding domains required for activation. Structure 16:1313-1323.

Seth A, Otomo C, Rosen MK. 2006. Autoinhibition regulates cellular localization and actin assembly activity of the diaphanous-related formins FRLalpha and mDia1. J Cell Biol 174:701-713.

Staus DP, Blaker AL, Medlin MD, Taylor JM, Mack CP. 2011. Formin homology domain-containing protein 1 regulates smooth muscle cell phenotype. Arterioscler Thromb Vasc Biol 31:360-367.

Tojo H, Kaieda I, Hattori H, Katayama N, Yoshimura K, Kakimoto S, Fujisawa Y, Presman E, Brooks CC, Pilch PF. 2003. The Formin family protein, formin homolog overexpressed in spleen, interacts with the insulin-responsive aminopeptidase and profilin IIa. Mol Endocrinol 17:1216-1229.

Wang J, Dube DK, White J, Fan Y, Sanger JM, Sanger JW. 2012. Clock is not a component of Z-bands. Cytoskeleton (Hoboken) 69:1021-1031.

Westendorf JJ. 2001. The formin/diaphanous-related protein, FHOS, interacts with Rac1 and activates transcription from the serum response element. J Biol Chem 276:46453-46459.

Westendorf JJ, Mernaugh R, Hiebert SW. 1999. Identification and characterization of a protein containing formin homology (FH1/FH2) domains. Gene 232:173-182.

Wilson AJ, Schoenauer R, Ehler E, Agarkova I, Bennett PM. 2014. Cardiomyocyte growth and sarcomerogenesis at the intercalated disc. Cell Mol Life Sci 71:165-181.

Yamaguchi M, Yamano S, Muguruma M, Robson RM. 1988. Polarity and length of actin filaments at the fascia adherens of the cardiac intercalated disk. J Ultrastruct Mol Struct Res 100:235-244.

Yoshida M, Sho E, Nanjo H, Takahashi M, Kobayashi M, Kawamura K, Honma M, Komatsu M, Sugita A, Yamauchi M, Hosoi T, Ito Y, Masuda H. 2010. Weaving hypothesis of cardiomyocyte sarcomeres: discovery of periodic broadening and narrowing of intercalated disk during volume-load change. Am J Pathol 176:660-678.

Figure legends

Figure 1: **Schematic representation of the domain layout of FHOD1 and the FHOD1 constructs used for transient transfection into NRC.** N-terminally GFP-tagged full length FHOD1 including (A) or lacking the

alternatively spliced exons 12 and 13 (B) and the respective deletion constructs (C-H). Domain borders are given in brackets. GBD GTPase binding domain, DID Diaphanous inhibitory domain, FH1 Formin homology domain 1, FH2 Formin homology domain 2, DAD Diaphanous autoregulatory domain.

Figure 2: **Evaluation of commercially available antibodies for their specificity to recognise FHOD1.** A) Confocal micrographs of transiently transfected COS cells either using GFP-FHOD1 (left column) or HA-FHOD3 (right column; green signal) and counterstaining with the different antibodies against FHOD1 (red signal). Only in the left column is yellow signal observed, indicating a specific reaction of the antibodies with FHOD1 and no crossreaction with its closest relative FHOD3. B) Immunoblot using the different anti FHOD1 antibodies on SDS samples from COS cells transiently transfected with GFP-FHOD1 (lane 1), HA-FHOD3 (lane 2) or untransfected COS cells (lane 3).

Figure 3: **The phosphoThr1141 FHOD1 antibody only detects overexpressed full length FHOD1 but not C-terminally truncated FHOD1.** Confocal micrographs of NRC transfected either with GFP-tagged full length FHOD1 (left column) or deltaDAD FHOD1 (right column).

Figure 4: **FHOD1 is expressed in the heart.** Immunoblot with pM anti FHOD1 shows a band with the expected molecular weight in mouse heart and

tibialis anterior (TA) and to a lesser extent in soleus (A). Immunoblotting with a pR antibody against sarcomeric alpha-actinin was used as a loading control for the striated muscle samples (B), spleen was used as a positive control for FHOD1 expression.

Figure 5: **FHOD1 is preferentially located at the intercalated disc.** Confocal micrographs of frozen sections of mouse heart stained with different antibodies against FHOD1. A) pG anti FHOD1 (C14), B) pG anti FHOD1 (C20), C) pR anti FHOD1 PhosphoThreonine 1141. All FHOD1 antibodies (red signal in merge) predominantly delineate the intercalated disc, in addition there is an occasional striated pattern apparent. Counterstaining with a mM against myomesin (green signal in merge), an M-band protein, suggests that this pattern may be Z-disc associated. The nuclei were stained with DAPI (blue signal in merge). Scale bar is equivalent to 10 micrometers.

Figure 6: **Expression test of different FHOD1 constructs in COS cells.** Immunoblot with GFP antibodies of SDS samples from COS cells that were transiently transfected with the different FHOD1 constructs. A) 12% SDS-PAGE, B) 7.5% SDS-PAGE. Constructs of the expected molecular weight were observed in all samples. Untransfected COS cells were used as a negative control (COS).

Figure 7: **Overexpressed FHOD1 is mainly located at the cellular periphery in NRC.** A) Confocal micrographs of NRC after transient

transfection with either GFP-tagged full length or B) GFP-tagged constitutively active (DeltaDAD) FHOD1 (green signal in merge), counterstained with mM antibodies against the Z-disc protein alpha-actinin (red signal in merge) and against F-actin (visualised with Alexa633-phalloidin, blue signal in merge). FHOD1 is mainly located in a diffuse fashion with marked concentration in the periphery of the cells. While expression of a constitutively active version of FHOD1 does not seem to perturb myofibrillar organisation too much, the cells have increased F-actin. Scale bar is equivalent to 10 micrometres.

Figure 8: **Subcellular targeting of GFP-tagged FHOD1 subdomains in NRC.** Confocal micrographs of NRC transfected with different GFP tagged fragments of FHOD1 (green signal in merge). Cells were counterstained with mM antibodies against sarcomeric alpha-actinin or myomesin (red signal in merge) and F-actin was visualised by Alexa633-phalloidin (blue signal in merge). A) FH2 domain [642-1031], B) GBD-DID [1-340], C) the GBD [1-116], D) DID [117-340], and E) FHOD1 (long version) lacking the GBD (DeltaGBD) [117-1191]. FH, formin homology; GBD, GTPase binding domain; DID, diaphanous inhibitory domain. Scale bar is equivalent to 10 micrometers. While the FH2 domain on its own targets to the Z-disc, GBD-DID and GBD show a diffuse localisation with some sarcomeric targeting. DID alone and an N-terminally truncated version of FHOD1 have lost all ability to target and are found in cytoplasmic aggregates (DID) or in a vesicular pattern (DeltaGBD), suggesting that the GBD domain may mediate the subcellular localisation of full length FHOD1. Scale bar is equivalent to 10 micrometres.

Figure 9: **FHOD1 is increased at the intercalated disc in DCM.** Confocal micrographs of murine (A, MLP KO mice) or human (B) DCM samples (left ventricle) in comparison with the respective wildtype or control heart tissue. A) FHOD1 was stained in red using a pG anti FHOD1, the M-bands were visualised with a mM anti myomesin (green signal in merge) and the intercalated discs were stained with pR antibodies against N-RAP (blue signal in merge). A) FHOD1 was stained in red using a pR anti FHOD1 PhosphoThreonine 1141 antibody and the M-bands were visualised with a mM anti myomesin (green signal in merge). The nuclei were stained with DAPI and are only shown in blue in the merge. Scale bar is equivalent to 10 micrometres.

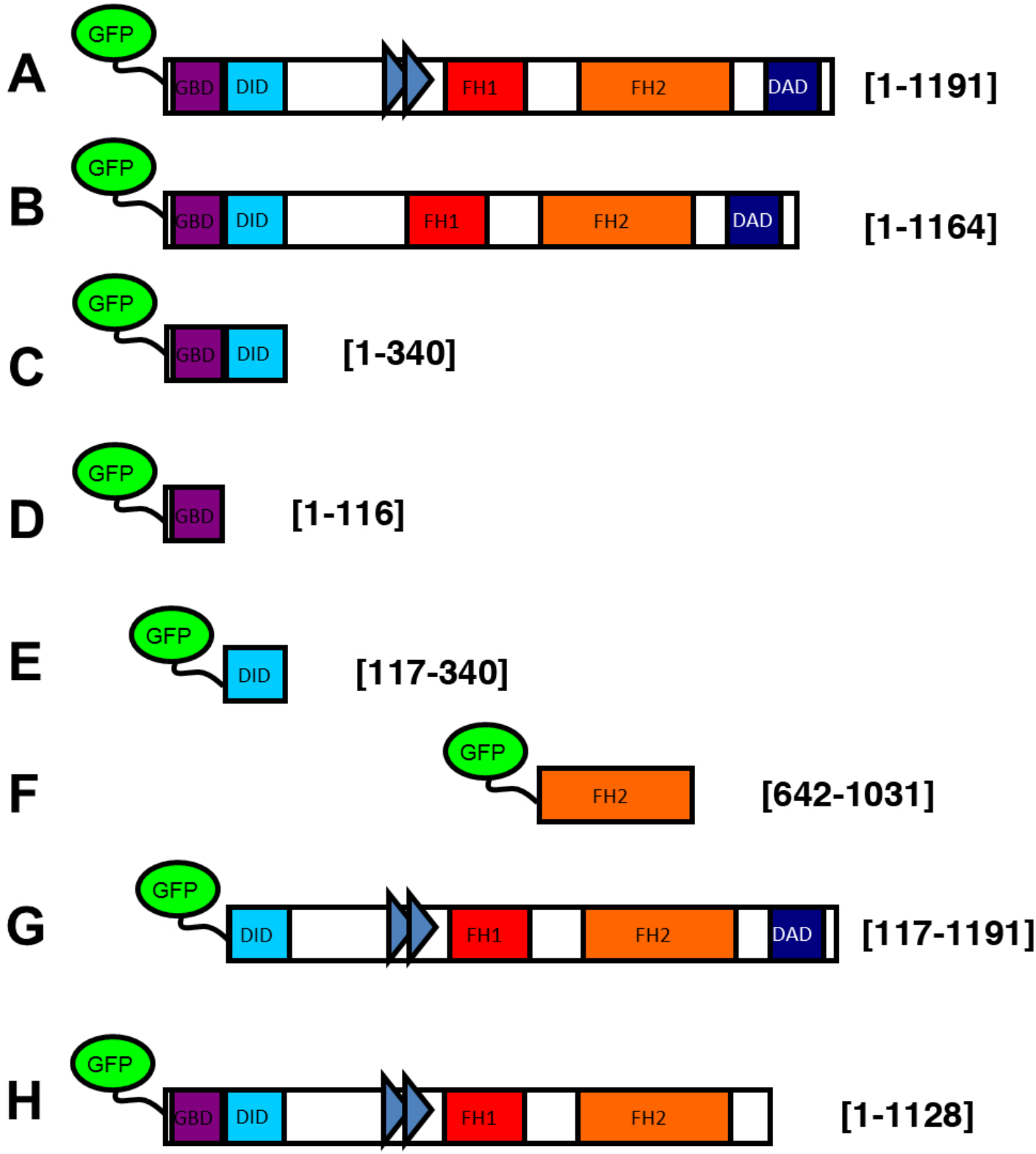
A
GFP
GBD
DID
FH1
FH2
DAD
[1-1191]
B
GFP
GBD
DID
FH1
FH2
DAD
[1-1164]
C
GFP
GBD
DID
[1-340]
D
GFP
GBD
[1-116]
E
GFP
DID
[117-340]
F
GFP
FH2
[642-1031]
G
GFP
DID
FH1
FH2
DAD
[117-1191]
H
GFP
GBD
DID
FH1
FH2
[1-1128]

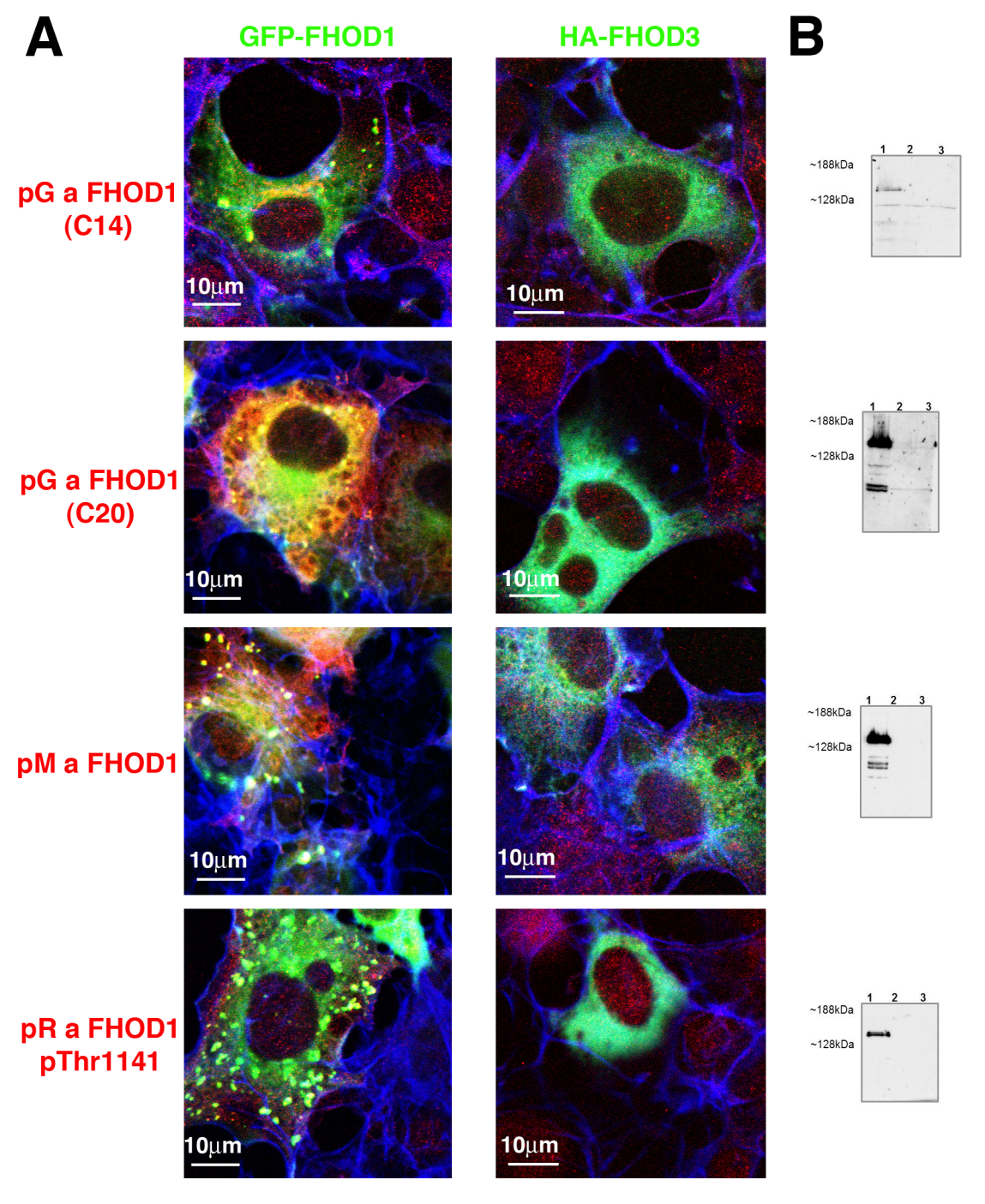
A
GFP-FHOD1
HA-FHOD3
B
pG a FHOD1 (C14)
pG a FHOD1 (C20)
pM a FHOD1
pR a FHOD1 pThr1141
10μm
1 2 3
~188kDa
~128kDa

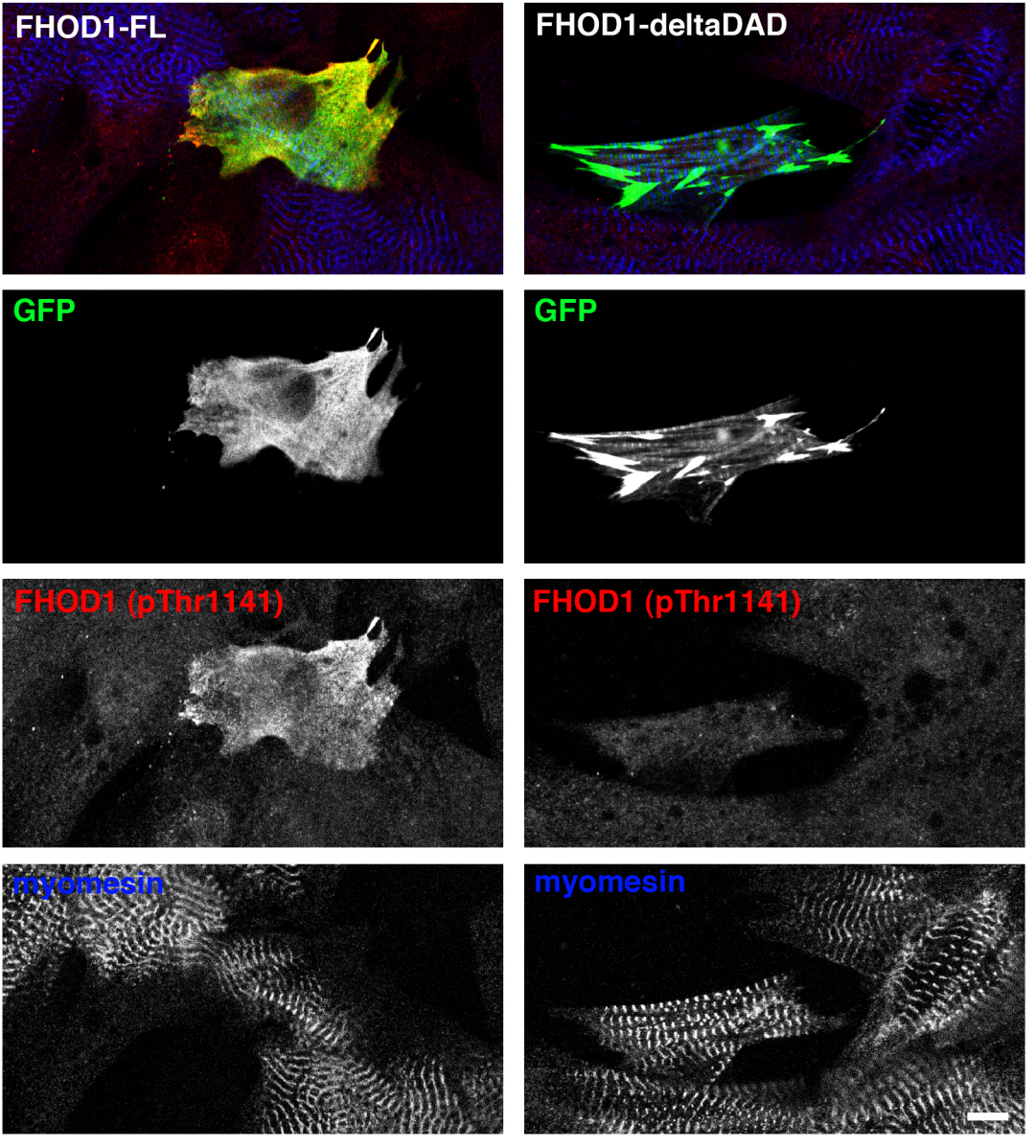
FHOD1-FL
FHOD1-deltaDAD
GFP
GFP
FHOD1 (pThr1141)
FHOD1 (pThr1141)
myomesin
myomesin

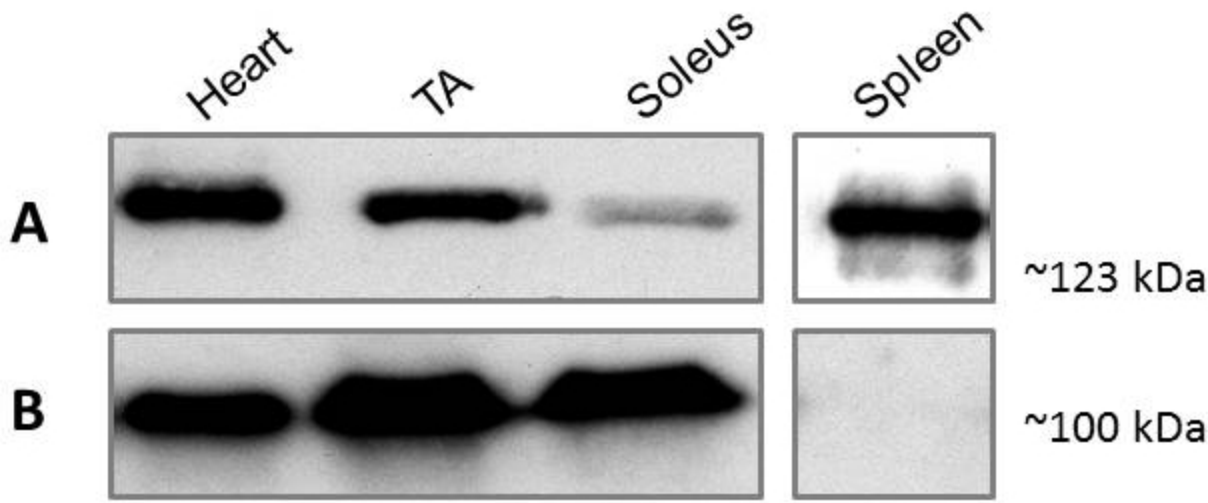
Heart
TA
Soleus
Spleen
A
B
~123 kDa
~100 kDa

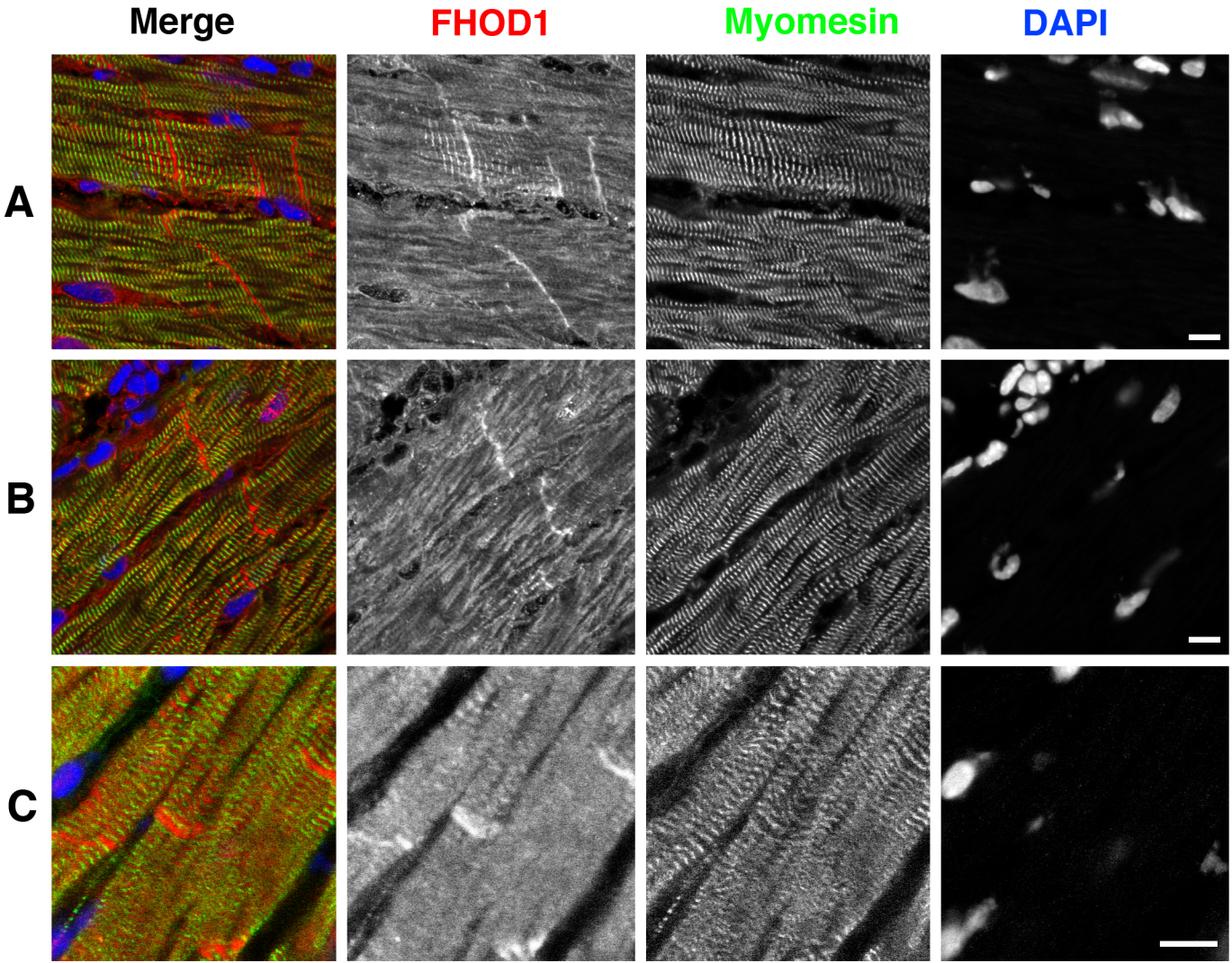
Merge
FHOD1
Myomesin
DAPI
A
B
C

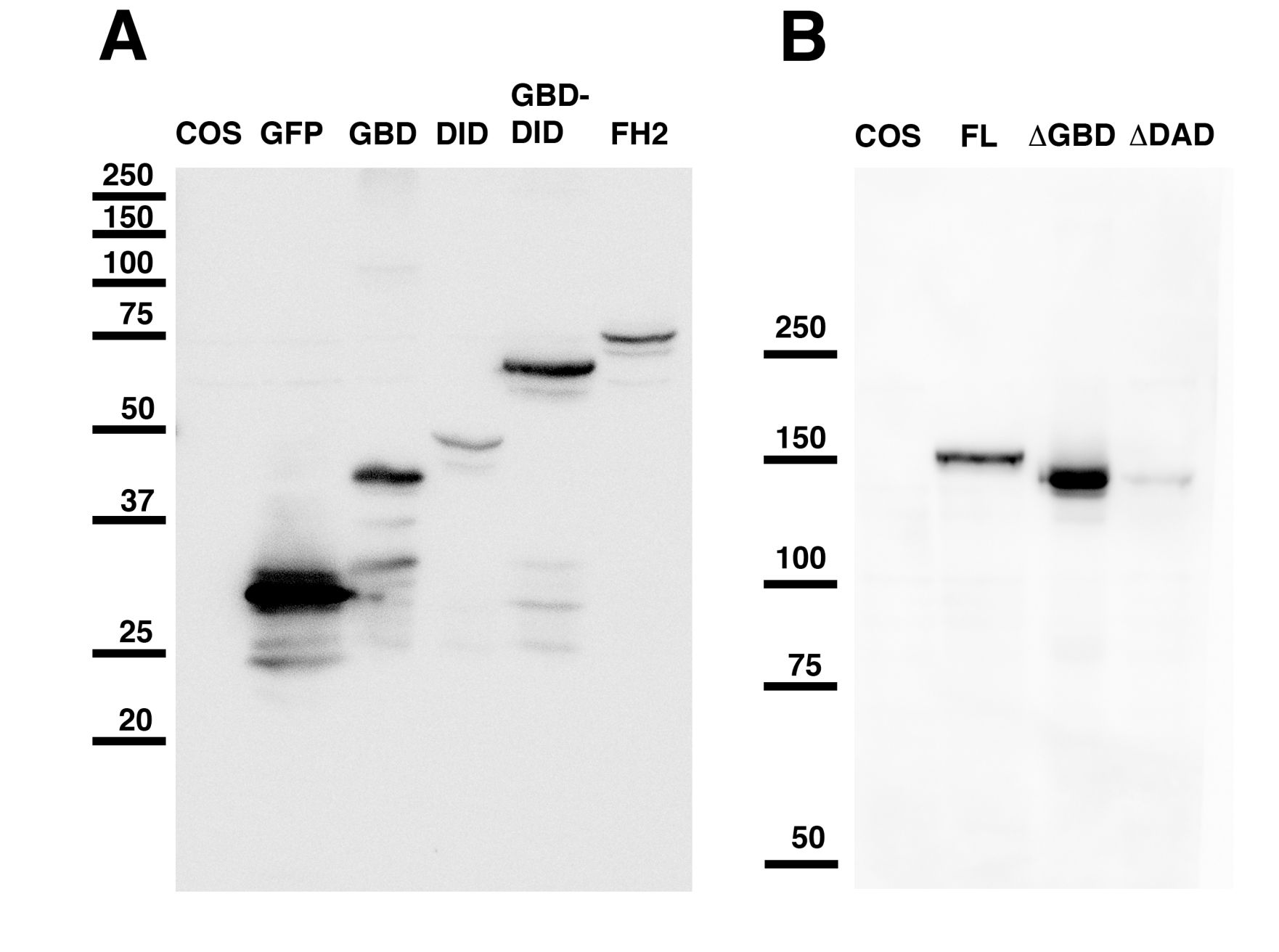
A
COS
GFP
GBD
DID
GBD-DID
FH2
250
150
100
75
50
37
25
20
B
COS
FL
ΔGBD
ΔDAD
250
150
100
75
50

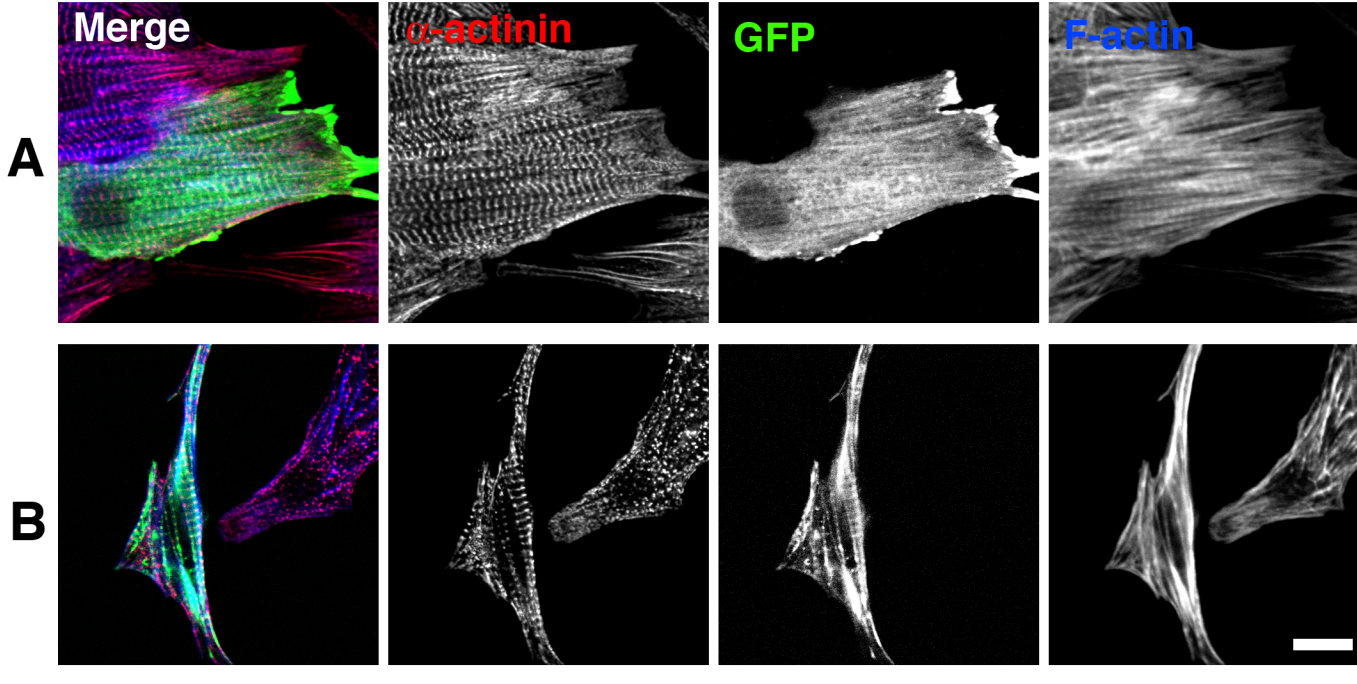
Merge
α-actinin
GFP
F-actin
A
B

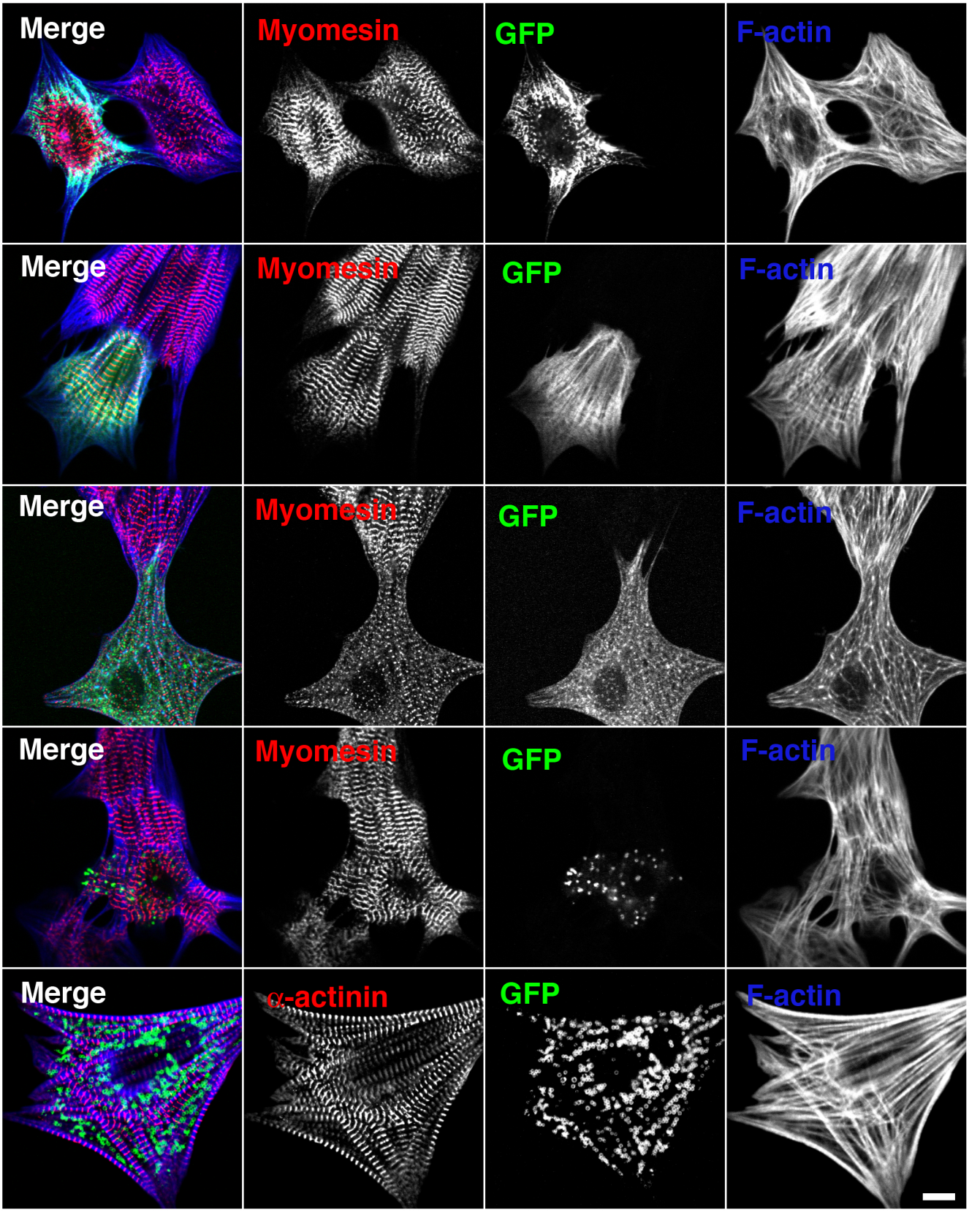
A
Merge
Myomesin
GFP
F-actin
B
Merge
Myomesin
GFP
F-actin
C
Merge
Myomesin
GFP
F-actin
D
Merge
Myomesin
GFP
F-actin
E
Merge
α-actinin
GFP
F-actin

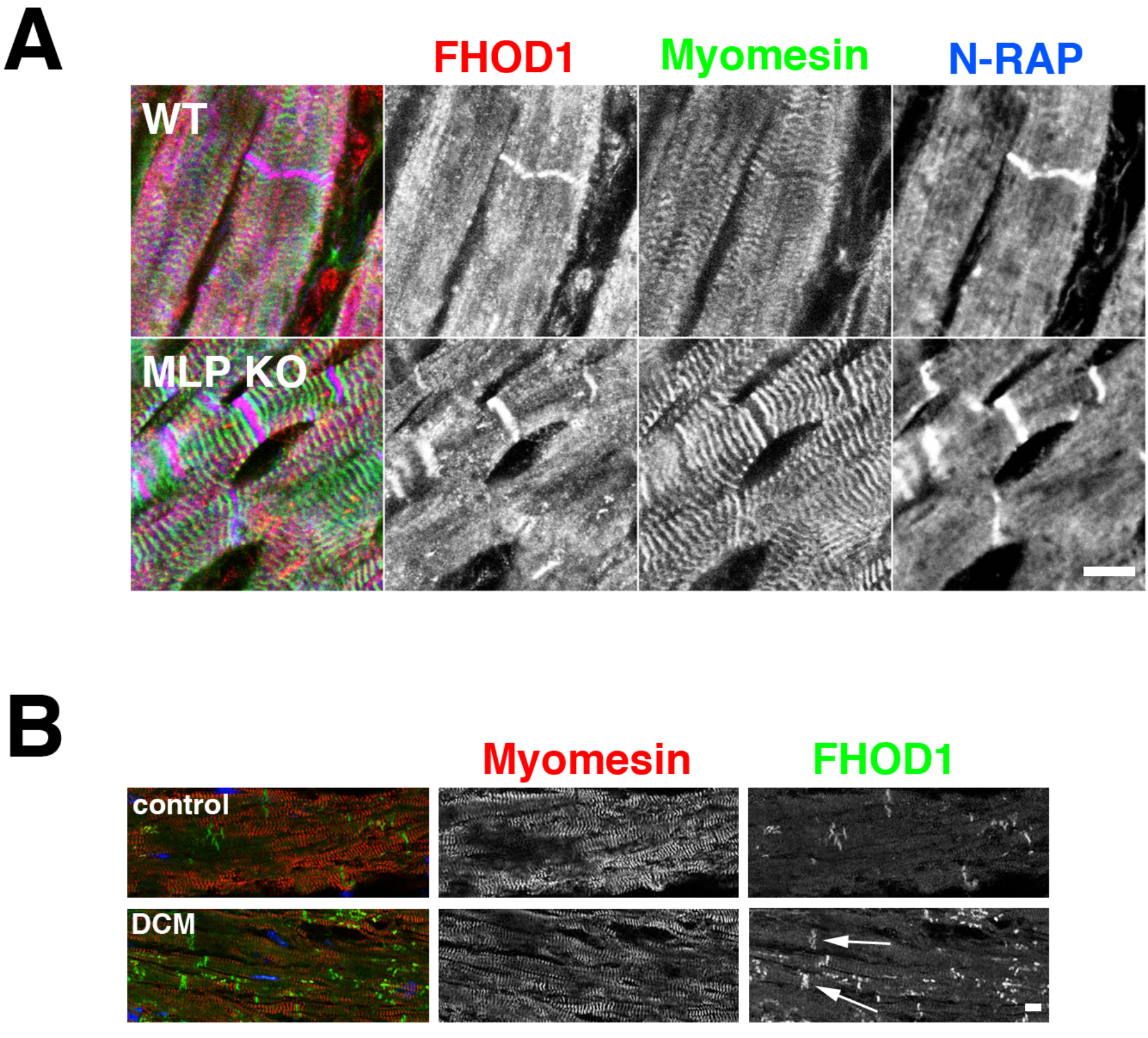
A
FHOD1
Myomesin
N-RAP
WT
MLP KO
B
Myomesin
FHOD1
control
DCM